Structure and Polyphenylvinylene Concentration Effect on the Photoconductivity Response from Mesostructured Silica Films

J. García M.,*,† G. Valverde,† D. Cruz,† A. Franco,† J. I. Zink,‡ and P. Minoofar‡

Instituto de Física, Universidad Nacional Autónoma de México, Apartado Postal 20-364, 01000 México D.F., and Department of Chemistry and Biochemistry, University of California at Los Angeles, 405 Hilgard Avenue, Los Angeles, California 90095

Received: November 8, 2002; In Final Form: November 27, 2002

Highly ordered thin films were made by a dip-coating technique. Sodium dodecyl sulfate (SDS)-templated sol−gel films possess lamellar structure, and cetyltrimethylammonium bromide-templated sol−gel films exhibit a hexagonal structure. In this work, mesostructured films made with these surfactants were doped with polyphenylvinylene (PPV). X-ray diffraction patterns indicate that the films have the known structure. The photoconductivity technique was used to determine the charge-transport mechanism on these films. The parameters for the photovoltaic effect (ϕl_0) and photoconductivity ($\phi\mu\tau$) were determined from the current density versus the applied-electrical-field results. Lamellar films have bigger values of these parameters than the corresponding ones from the hexagonal films, and the conductivity is better in the former. Charge-transport parameters are quite high in the PPV-doped samples compared with the reported values in films doped with Disperse Red 1 and carbazole (SiK). $KNbO_3:Fe^{3+}$ photorefractive crystals are less photoconductive and photovoltaic than the PPV films, too. There is a critical polymer concentration in the SDS samples.

Introduction

Recent developments in the preparation of mesostructured templated sol−gel silica materials have extended the morphology from the originally discovered powders, with particle sizes on the order of microns,[1,2] to continuous thin films.[3] To synthesize mesostructured silica thin films, four reagents are generally required: water, a surfactant, a silica source (such as tetraethyl orthosilicate or tetramethyl orthosilicate), and a catalyst.

Mesostructured silica thin films use surfactants to template or provide ordered structure to the amorphous silica matrix. The mesostructured thin films consist of two regions: the "framework" that is formed by the sol−gel metal oxide and the "organic" region that is formed by the template.[4]

It is well-known that sodium dodecyl sulfate (SDS)-templated mesostructured sol−gel thin films produced by a dip-coating method possess a highly ordered lamellar structure.[5,6] In solution, the cationic surfactant cetyltrimethylammonium bromide (CTAB) forms several mesophases as the CTAB concentration increases. CTAB first forms spherical micelles and then micellar rods. These micellar rods organize into a hexagonal structure, followed by the transformation to a cubic and finally lamellar phase as the surfactant concentration continues to increase.[7,8] Films made by dip coating with 3.5 wt % CTAB form the hexagonal phase at a low withdrawal speed.[9]

Carbazole and Disperse Red 1 (DR1) have been incorporated in amorphous materials for nonlinear optical phenomena such as linear electrooptic, nonlinear optical, and photorefractive effects.[10] The possibility of tailoring the functionality of mesostructured silica films allowed the incorporation of the charge-transporting molecule (carbazole) and the second-order chromophore (DR1) in SDS-templated films. In these films, the DR1 molecules were oriented by a corona discharge. Photoconductivity studies were made on these films to know their charge-transport parameters as a function of the polarization state.[4,11]

The nonlinear optical response depends drastically on the charge transport inside the material. It is extremely important to study the conductivity on the samples under dark and illuminated conditions to obtain the charge-transport parameters. To have a material with useful and highly efficient nonlinear optical properties, the dopant molecules need to exhibit large second-order molecular hyperpolarizabilities, which can result from a highly extended π-conjugated core with an electron donor−acceptor pair at the ends. Furthermore, the external electrical orientation of these molecules allows for the obtainment of a noncentrosymmetric material such that the molecular contribution can be maximized in the material.[12]

In this paper, we report for the first time the development of mesostructured sol−gel silica thin films doped with a conducting polymer, PPV, and templated with SDS or CTAB. We perform photoconductivity studies on them. The charge-transport parameters were calculated and compared with those reported from SDS-templated films doped with DR1 and carbazole and $KNbO_3:Fe^{3+}$ photorefractive crystals.

Experimental Section

Precursor solutions were prepared by the addition of two cationic surfactants (SDS, $C_{12}H_{25}O_4SNa$; CTAB, $CH_3(CH_2)_{15}N^+(CH_3)_3Br^-$) to polymeric silica solutions (A2**) made by a two-step process[13] that was designed to minimize the siloxane condensation rate,[14] thus promoting facile silica−surfactant coassembly during film deposition. First, tetraethyl orthosilicate [$Si(OC_2H_5)_4$], ethanol, deionized water, and 0.07 N HCl (molar

* Corresponding author. E-mail: gamaj@fisica.unam.mx. Phone: (5255)-56-22-51-03. Fax: (5255)56-16-15-35.
† Universidad Nacional Autónoma de México.
‡ University of California at Los Angeles.

10.1021/jp0274132 CCC: $25.00
Published on Web 02/11/2003

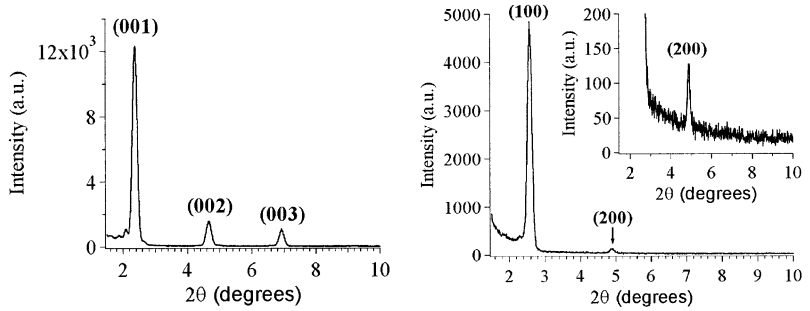

Figure 1. (a) XRD patterns at low angle of film with SDS:P255 = 1:4 × 10^{-6} M. (b) XRD patterns of film with CTAB:P255 = 1:60 × 10^{-6} M. The inset is the enlargement of the (200) peak.

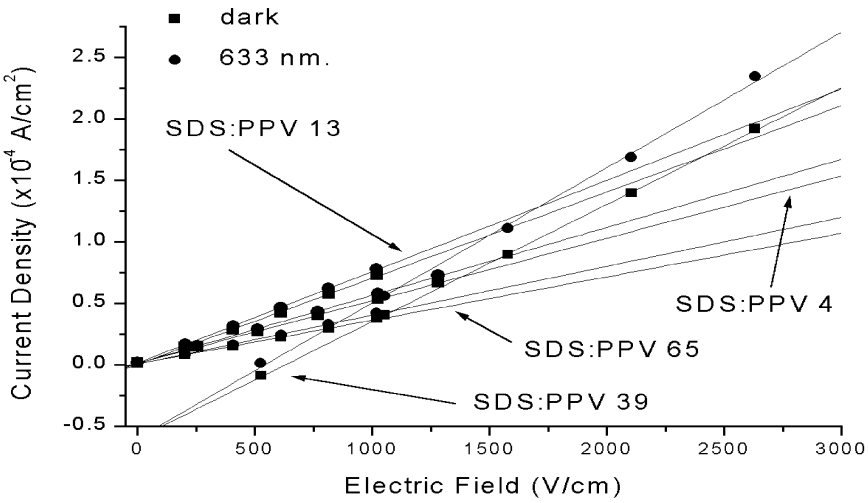

Figure 2. Dark and 633-nm illumination current curves for different P255 molar concentrations (listed in Table 1) in samples with 1.5% SDS.

TABLE 1: Molar Concentrations of PPV Added to the Surfactant

SDS	P255	CTAB	P255
1	4×10^{-6}	1	8×10^{-6}
1	13×10^{-6}	1	39×10^{-6}
1	39×10^{-6}	1	60×10^{-6}
1	65×10^{-6}		

ratio: 0.14:0.52:0.13:3 × 10^{-3}) were refluxed at 60 °C for 90 min to obtain a stock solution (A2**). Second, 0.4 mL of water and 1.2 mL of HCl were added to 10 mL of A2**, and the solution was stirred for 10 min. Then, 23 mL of ethanol was added followed by the polymer P255 (or PPV) at different molar concentrations (see Table 1). The solution was stirred for 10 min. Finally, the surfactant was added to this solution using 3.5% CTAB or 1.5% SDS. The solution was stirred for 3 days at room temperature. P255 was prepared by mixing 0.1 mL of P255 (3% in concentration) in 4 mL of methanol.

The glass substrates were cleaned with sulfuric acid/H_2O_2 (4:1) and heated and stirred for 0.5 h. They were then placed in deionized water and boiled for 0.5 h, rinsed three times with deionized water, and stored in deionized water at room temperature. The films were deposited on the glass substrates (9 cm × 1 cm × 1 mm). The films were drawn with the equipment described previously that uses hydraulic motion to produce a steady and vibration-free withdrawal of the substrate from the solution.[15] The films were produced by dip coating at a constant withdrawal rate of 5.68 cm/min.

The structures of the final films were characterized with X-ray diffraction (XRD) using a Siemens D500 diffractometer. Optical absorption spectra were taken with a Lambda 900 Perkin-Elmer spectrophotometer.

For the photoconductivity studies,[11] the silver electrodes were painted on the sample. It was maintained in a 10^{-5}-Torr vacuum cryostat at room temperature to avoid humidity. For the photocurrent measurements, the films were illuminated with light from an Oriel Xe lamp passed through a 0.25-m Spex monochromator. Currents were measured with a 642 Keithley electrometer connected in series with the voltage power supply. The applied electrostatic field *E* was parallel to the film. The light intensity was measured at the sample position with a Spectra Physics 404 power meter.

Results

Figure 1 shows the low-angle XRD pattern for our films with P255. Figure 1a corresponds to the film with a lamellar phase (SDS),[4−6] and Figure 1b corresponds to the film with hexagonal structure, resulting from CTAB tubes.[9]

Figure 2 shows the photoconductivity results from the films with 1.5% SDS and different P255 concentrations. The data were linearly fitted by the least-squares method. They show a linear current-density dependence with the applied electric field, which means they exhibit an ohmic behavior. As shown, the current increases with PPV concentration until a maximum response is reached. At higher concentration, the current density diminishes.

The photoconductivity results from films with 3.5% CTAB are shown in Figure 3. They exhibit an ohmic behavior, too. In this case, the response is clearly dependent on PPV concentration and illumination, in contrast with the lamellar case. There is a

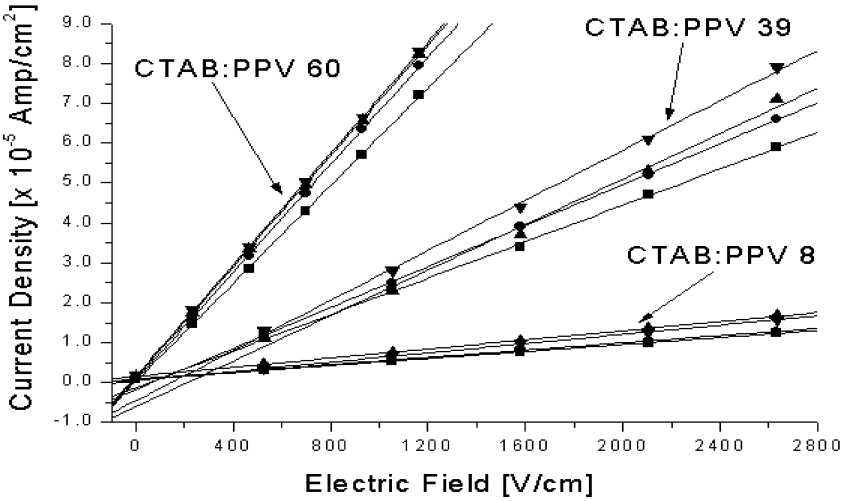

Figure 3. Dark and illuminated current curves for different PPV molar concentrations (listed in Table 1) in samples with 3.5% CTAB.

TABLE 2: Charge-Transport Parameters

sample		$\lambda = 633$ nm	$\lambda = 515$ nm	$\lambda = 488$ nm
PPV:SDS 4×10^{-6}	ϕl_0 (cm)	5.9×10^{-8}	3.7×10^{-8}	1.2×10^{-7}
	$\phi\mu\tau$ (cm^2/V)	1.2×10^{-9}	3.7×10^{-9}	3.9×10^{-9}
PPV:SDS 13×10^{-6}	ϕl_0 (cm)	1.0×10^{-6}	2.7×10^{-7}	2.2×10^{-7}
	$\phi\mu\tau$ (cm^2/V)	4.0×10^{-9}	2.6×10^{-9}	1.8×10^{-9}
PPV:SDS 39×10^{-6}	ϕl_0 (cm)	1.2×10^{-7}	1.6×10^{-6}	2.0×10^{-6}
	$\phi\mu\tau$ (cm^2/V)	1.8×10^{-9}	1.0×10^{-9}	1.1×10^{-9}
PPV:SDS 65×10^{-6}	ϕl_0 (cm)	4.3×10^{-8}	1.0×10^{-8}	1.6×10^{-8}
	$\phi\mu\tau$ (cm^2/V)	1.3×10^{-9}	6.6×10^{-10}	9.5×10^{-10}
PPV:CTAB 8×10^{-6}	ϕl_0 (cm)	2.2×10^{-8}	2.2×10^{-6}	3.1×10^{-8}
	$\phi\mu\tau$ (cm^2/V)	1.5×10^{-11}	3.3×10^{-9}	1.6×10^{-10}
PPV:CTAB 39×10^{-6}	ϕl_0 (cm)	2.3×10^{-7}	3.2×10^{-7}	1.7×10^{-7}
	$\phi\mu\tau$ (cm^2/V)	1.4×10^{-9}	3.3×10^{-10}	4.1×10^{-10}
PPV:CTAB 60×10^{-6}	ϕl_0 (cm)	1.3×10^{-7}	6.6×10^{-8}	9.2×10^{-8}
	$\phi\mu\tau$ (cm^2/V)	2.4×10^{-9}	6.2×10^{-10}	6.6×10^{-10}
SDS:DR1:SiK (ref 4)	ϕl_0 (cm)	6.63×10^{-11}		
	$\phi\mu\tau$ (cm^2/V)	0.23×10^{-11}		
$KNbO_3$:Fe^{3+} (ref 11)	ϕl_0 (cm)	0.85×10^{-8}	0.10×10^{-8}	0.58×10^{-8}
	$\phi\mu\tau$ (cm^2/V)	23.38×10^{-11}	4.52×10^{-11}	7.14×10^{-11}

dramatic change in the slopes with concentration. The straight lines from CTAB:PPV 39×10^{-6} M in Figure 3 correspond in ascending order to dark conditions (■) and illumination at 633 nm (●), 515 nm (▲), and 488 nm (▼), respectively. This means that the slope from these lines increases with the illumination energy. The same results are obtained for the other two concentrations. To avoid confusion, in the SDS samples in Figure 2 we show for each concentration only the results obtained under dark and 633-nm illumination conditions.

The slopes from Figures 2 and 3 versus PPV concentration are plotted in Figure 4. It is observed that the slopes increase with the PPV concentration and illumination energy, for both surfactants, up to the critical concentration $= 39 \times 10^{-6}$ M. As is observed, this is an optimal P255 concentration in the SDS samples, because at higher concentrations the slopes diminish. Also, Figure 1 confirms that for this concentration we obtain the highest current. In general, the slopes from the SDS films are larger than those from the CTAB films, and a comparison of Figures 2 and 3 clearly shows that in lamellar samples conduction is 3 times that obtained from hexagonal samples. This means that the tubes have restrictions to conduction, which diminishes the transport, as is clearly observed in Figure 4. In this last case, there are probably too many PPV chains, some inside the tubes and others outside, such that interchain interaction interrupts the linear conduction, in the reverse way to the behavior from the chains in the planes at concentrations less than the critical concentration. We think the critical

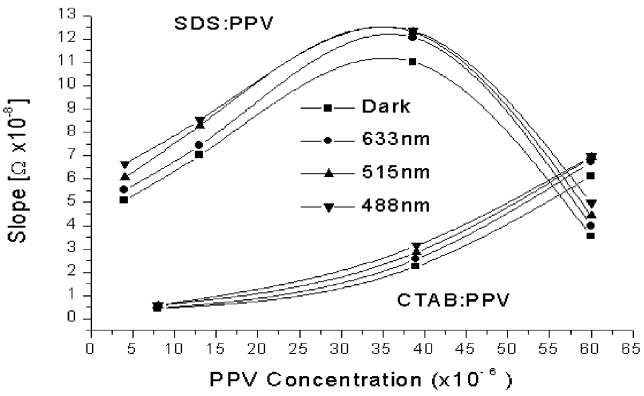

Figure 4. Slope dependence on the PPV concentration and illumination.

concentration in the SDS samples is due to the fact that the P255 chains are too long, and when the concentration is too high, the chains become so cross-linked that conduction is diminished, too.

Charge transport in insulating materials is given by[11]

$$j = e\phi l_0 \alpha I/h\nu + (en_0\mu + e\phi\mu\tau\alpha I/h\nu)E$$

The first term is the photovoltaic-effect transport, the second is the dark conductivity $\sigma = en_0\mu$, and the third is the photocon-

ductivity itself. In this equation, I is the light intensity with energy $h\nu$, ϕ is the quantum efficiency for exciting a free carrier, μ is the charge mobility, E is the applied electric field, α is the absorption coefficient, τ is the half-life of the excited carriers, n_0 is the carrier density that produces dark conductivity, and l_0 is the mean free path. With this equation, by measuring I, the dark conductivity, and the conductivity under illumination and fitting the data by the least-squares method as shown in Figure 3, the ϕl_0 and $\phi\mu\tau$ parameters are obtained. They are reported in Table 2. ϕl_0 is related to how photovoltaic the material is, that is, how strong the induced voltage is under illumination. $\phi\mu\tau$ is related to how photoconductive the material is, that is, how much conduction is produced under illumination, compared with the dark response.

Table 2 shows that in the SDS samples ϕl_0 initially increases with the PPV concentration and then decreases, but $\phi\mu\tau$ decreases with concentration. In the CTAB samples, ϕl_0 does the same, but $\phi\mu\tau$ increases with concentration, at least under 488- and 633-nm illumination. Comparing the results from SDS and CTAB samples with similar PPV concentrations (39×10^{-6} M in both or 13×10^{-6} and 8×10^{-7} M), we see that the photovoltaic and photoconductive responses are bigger in the planes (SDS) than in the tubes (CTAB).

The conduction parameters are quite high in all the PPV samples compared with SDS films doped with the DR1 chromophore and carbazole. This confirms the contribution of PPV to the photoconductivity. Our results with $KNbO_3:Fe^{3+}$ photorefractive crystals show that this material is less photovoltaic and photoconductive than PPV films.

Conclusions

The produced films exhibit a highly ordered hexagonal and lamellar structure. Films with lamellar structure have better photoconductivity than films with hexagonal structure, but the concentration effect is more noticeable in the hexagonal ones. In SDS films, there is an optimal P255 concentration at which the conductivity reaches the highest value. We think the polymer's chains interact too strongly and that this represents a barrier for charge transport in the CTAB samples and in the lamellar samples at high PPV concentration. The photovoltaic and photoconductive values are bigger in the planes (SDS) than in the tubes (CTAB). The charge carrier parameters in the PPV films are quite big compared with the lamellar films doped with DR1. The $KNbO_3:Fe^{3+}$ crystals are less photovoltaic and photoconductive than the mesostructured films doped with PPV.

Acknowledgment. This work has been supported by UC-MEXUS, DGAPA UNAM IN103199, and CONACYT 34582E.

References and Notes

(1) Kresge, C. T.; Leonowicz, M. E.; Roth, W. J.; Vartuli, J. C.; Beck, J. S. *Nature (London)* **1992**, *359*, 710.

(2) Beck, J. S.; Vartuli, J. C.; Roth, W. J.; Leonowicz, M. E.; Kresge, C. T.; Schmitt, K. D.; Chu, C. T.-W.; Olson, D. H.; Sheppard, E. W.; McCullen, S. B.; Higgins, J. B.; Schlenker, J. L. *J. Am. Chem. Soc.* **1992**, *114*, 10834.

(3) Tolbert, S. H.; Schäffer, T. E.; Feng, J.; Hansma, P. K.; Stucky, G. D. *Chem. Mater.* **1997**, *9*, 1962.

(4) García M., J.; Cruz, D.; Valverde, G.; Zink, J. I.; Hernandez, R. *J. Sol.-Gel Sci. Technol.* **2003**, *26*, 1.

(5) Huang, M. H.; Dunn, B. S.; Zink, J. I. *J. Am. Chem. Soc.* **2000**, *122*, 3739.

(6) Huang, M. H.; Dunn, B. S.; Soyez, H.; Zink, J. I. *Langmuir* **1998**, *14*, 7331.

(7) Ross, S.; Morrison, I. D. *Colloid Systems and Interfaces*; John Wiley & Sons: New York, 1988; p 173.

(8) Raman, N. K.; Anderson, M. T.; Brinker, C. J. *Chem. Mater.* **1996**, *8*, 1682.

(9) Yunfeng, L.; et al. *Nature* **1997**, *389*, 364.

(10) Chaput, F.; Riehl, D.; Boilot, J. P.; Cargnelli, K.; Canva, M.; Levy, Y.; Brun, A. *Chem. Mater.* **1996**, *8*, 312.

(11) García M., J.; Mondragon, M. A.; Hernandez, J. M.; Maldonado, J. L. *Opt. Mater.* **1994**, *3*, 61.

(12) Williams, D. J. *Angew. Chem., Int. Ed. Engl.* **1984**, *23*, 690.

(13) Brinker, C. J.; et al. In *Access in Nanoporous Materials*; Pinnavia, T. J., Thorpe, M. F., Eds.; Plenum: New York, 1995; p 123.

(14) Brinker, C. J.; Scherer, G. W. *Sol-Gel Science*; Academic: San Diego, 1996; p 120.

(15) Nishida, F.; McKierman, J. M.; Dunn, B.; Zink, J. I.; Brinker, C. J.; Hurd, A. J. *J. Am. Ceram. Soc.* **1995**, *78*, 1640.